Propagation of solitons in hydrogen-bonded chains with mass variation

G. Kalosakas, A. V. Zolotaryuk,* G. P. Tsironis, and E. N. Economou
Physics Department, University of Crete and Research Center of Crete/FORTH, P.O. Box 2208, 71003 Heraklion, Crete, Greece
(Received 17 January 1997)

In the context of the soliton mechanism for proton transport in hydrogen-bonded networks we analyze properties of kink propagation through disordered hydrogen-bonded chain when realistic mass variation along the chain is created through deuterium substitutions. We provide an interpretation for the kink propagation in the chain as the motion of a particle with variable mass. We show that mass impurity localized modes are excited only above a certain threshold of kink velocity and, as a result, the presence of mass impurities renormalizes the maximal kink velocity in the medium. The existence of a critical kink velocity for the excitation of impurity mode appears also in the study of the interaction of kink with a single impurity. [S1063-651X(97)02207-1]

PACS number(s): 42.65.Tg, 63.20.Ry, 63.20.Pw

I. INTRODUCTION

The basic idea in the soliton model of proton transport along a hydrogen-bonded chain (HB) stems from the fact that the proton in each H bond of the chain can be found in two equilibrium positions separated by a potential barrier. As a result, two degenerate HB ground states can be formed, viz. $\cdots$ X—H $\cdots X$—H $\cdots X$—H $\cdots$ and $\cdots$ H—$X\cdots$ H—$X\cdots$ H—$X\cdots$ [1], while the transitions between these two states in the displacive limit result in topological solitons [2–4]. When we consider only the ionic defect motion, the on-site potential of the HB proton can be constructed as the sum of two pair of ion-proton potentials, e.g., the Morse potentials [5]. In the study of the more general problem of ionic and orientational defects we can use appropriate doubly periodic functions that are known to simulate well the effective proton potential [6–9].

A progressively realistic study, in the context of soliton models, of proton motion in HB chains, has to address the effects in proton soliton (kink) motion of the presence of impurities in the system. Even though there exists work on the scattering properties of solitons, mainly from a single impurity [10–14], as well as rich literature on the nontopological soliton propagation in disordered media [15–20], there is no detailed knowledge regarding the more realistic situation of proton kink propagation in *long disordered* chains. This situation, that arises in HB chains doped with *deuterium* atoms, is currently addressed experimentally [21]. In order to analyze phenomena that are generated experimentally in the context of isotopic substitution and to investigate the proton-kink dynamics in the context of similarly produced disordered chains, we consider an HB chain with a binary mass variation. The mass m_n at given site n takes the values $m_n = m_p$ or $m_n = 2m_p$ depending on whether that site is occupied by a proton with mass m_p or a deuteron of mass $2m_p$, respectively.

The paper is organized as follows: In the Sec. II we present the soliton-bearing model with the inclusion of mass disorder. The properties of soliton propagation in a long mass-disordered segment are described in Sec. III. In the Sec. IV we develop a collective coordinate approach which allows us to interpret the numerical results of Sec. III. Concluding remarks are in Sec. V.

II. THE MASS-DISORDERED KINK-BEARING MODEL

The Hamiltonian for the complete chain can be written in the form

$$H=\sum_n \left[\frac{1}{2}\left(\frac{p_n^2}{m_n}\right)+\frac{1}{2}\kappa(u_{n+1}-u_n)^2+\varepsilon_0 V(u_n/l)\right], \quad (1)$$

where u_n is the displacement of the nth proton from the barrier top of the on-site potential $\varepsilon_0 V$ which is assumed to have, at least, two degenerate minima, compatible with a standard kink-bearing model [3,4], ε_0 is the height of the barrier between the minima of the on-site potential, $p_n=m_n du_n/dt$ is the nth proton momentum, κ is the stiffness constant of intersite proton-proton interaction, and l is the lattice spacing of the chain. The bistable (or multistable) function $V(q)$ is renormalized according to $V(q_1)=V(q_2)=0$ and $V(0)=1$, where q_1 and q_2 are the positions of the two minima around the origin $q=0$. It is convenient to use a dimensionless form of the Hamiltonian (1) and the corresponding equations of motion; this is accomplished by introducing the dimensionless time $\tau=(\kappa/m_p)^{1/2}\ t$, where m_p is the proton mass. Then the set of coupled equations of motion takes the form

$$\mu_n \ddot{q}_n = q_{n+1}-2q_n+q_{n-1}-\epsilon_0 V'(q_n), \quad n=0,\pm 1,\ldots, \quad (2)$$

where the lattice displacement field q_n is given in units of the lattice spacing l, i.e., $q_n(\tau)=u_n(\tau)/l$. Here $\mu_n=m_n/m_p$ describes the relative mass variation along the chain and $\epsilon_0=\varepsilon_0/\kappa l^2$ is the dimensionless potential barrier height. From here onwards the dot denotes the differentiation with respect to the dimensionless time τ and the prime will stand for spatial or other types of differentiation.

*Also at the Bogolyubov Institute for Theoretical Physics, 252 143 Kyiv, Ukraine.

In the continuum limit ($x=n$), the lattice field $q_n(\tau)$ and the mass distribution μ_n are substituted by $q(x,\tau)$ and $\mu(x)$, respectively. The dimensionless Lagrangian (in units of κl^2) has the form

$$\mathcal{L}=\int dx\left[\frac{1}{2}\mu(x)q_\tau^2-\frac{1}{2}q_x^2-\epsilon_0 V(q)\right]. \tag{3}$$

The corresponding equations of motion (2) take the form of the partial-differential equation

$$\mu(x)q_{\tau\tau}-q_{xx}+\epsilon_0 V'(q)=0, \tag{4}$$

which admits the standing soliton (kink and antikink) solution $q=q_K(x)$ given by the equations

$$q_K'(x)=\pm\sqrt{2\epsilon_0 V[q_K(x)]}\quad\text{or}\quad x=\pm\int_0^{q_K}\frac{dq}{\sqrt{2\epsilon_0 V(q)}}, \tag{5}$$

where the upper (lower) sign corresponds to a kink (antikink). As follows from these equations, the *standing* kink profile $q_K(x)$ does not depend on the mass variation $\mu(x)$.

In the particular case where there is no mass variation, i.e., $\mu(x)=1$, the time-dependent Eq. (4) has the ''relativistically'' covariant form and, therefore, the stationary soliton profile for the moving kink (and antikink) with the dimensionless speed $s=v/c_0$, where $c_0=\sqrt{\kappa/m_p}\ l$ is the characteristic velocity of proton sound, can be constructed from the static profile $q_K(x)$ by the substitution of the argument x by $\xi=(x-s\tau)/\sqrt{1-s^2}$. In the general case with mass variation, we assume the *same* dependence of the soliton profile on the position of its center $X=X(\tau)$ and the velocity $\dot{X}=\dot{X}(\tau)$, i.e., we substitute: $s\tau\to X(\tau)$ and $s\to\dot{X}(\tau)$, so that

$$q_K(x,\tau)=q_K(\xi),\quad \xi=\xi(x,\tau)=\frac{x-X(\tau)}{\sqrt{1-\dot{X}^2(\tau)}}, \tag{6}$$

may be considered as an approximate (see, e.g., Ref. [22]) soliton solution of Eq. (4) given in terms of the collective coordinate $X(\tau)$.

III. KINK PROPAGATION IN A MASS-DISORDERED SEGMENT

Using the ansatz given by Eqs. (6), for sufficiently small soliton velocities ($s^2\ll 1$) we can approximately write

$$q\simeq q_K(x-X),\quad q_\tau\simeq-\dot{X}q_K'(x-X),\quad q_x\simeq q_K'(x-X). \tag{7}$$

Substituting Eqs. (7) into the Lagrangian (3), we find for small velocities

$$\mathcal{L}=\mathcal{L}(\dot{X},X)=\tfrac{1}{2}M\dot{X}^2-E_0, \tag{8}$$

where

$$M=M(X(\tau))=\int F^2(x-X(\tau))\mu(x)dx \tag{9}$$

is the effective soliton mass and

$$E_0=M_0=\int F^2(x)dx=\int_{q_1}^{q_2}\sqrt{2\epsilon_0 V(q)}dq \tag{10}$$

is the rest soliton energy which in the dimensionless units is the same as the rest effective mass M_0. Here the function F has a bell-shaped form; it is defined through a soliton solution by

$$F(x)=|q_K'(x)|. \tag{11}$$

For simplicity of notations, we assume throughout this paper that the on-site potential $V(q)$ is a symmetric function. Therefore, $q_K\prime(-x)=q_K\prime(x)$. The form of the Lagrangian (8) allows us to interpret the motion of a topological soliton (kink or antikink) in a mass-disordered kink-bearing chain as the motion of an *effective particle with varying mass*. The total energy of the effective particle, whom its dynamics is described by the Lagrangian (8), is an integral of motion, i.e.,

$$E=E_0+\tfrac{1}{2}M(\tau)\dot{X}^2=\text{const}, \tag{12}$$

where the varying mass $M(\tau)$ is given by Eq. (9).

Next, we assume that the disordered chain segment is embedded in a regular chain with $m\equiv m_p$ and consider an incoming kink with an initial velocity $s_i=v_i/c_0$ from the regular part of the chain. Then its initial energy in the nonrelativistic limit is $M_0 s_i^2/2$ and, as a result, from Eq. (12) we find the time dependence of the velocity

$$\dot{X}(\tau)=\left(\frac{M_0}{M_0+\delta M(\tau)}\right)^{1/2}s_i,$$

$$\delta M(\tau)=\int F^2(x-X(\tau))\delta\mu(x)dx, \tag{13}$$

where we have represented the mass distribution $\mu(x)$ as the sum $\mu(x)=1+\delta\mu(x)$ with the continuum mass variation $\delta\mu(x)$. The sign of the kink acceleration at each instant of time τ depends on the sign of $\delta M(\tau)$ at this moment. Here $\delta M(\tau)$ can be considered as an increase or decrease of the effective rest mass M_0. In the particular case when deuteriums are present in the chain, we have a positive stochastically varying (in time) kink mass. A kink entering the disordered segment with a small initial velocity s_i and while propagating in it experiences a random reduction of its velocity. The equation of motion (13) predicts that upon exiting the segment, the final kink velocity s_f is the same as the initial velocity s_i. In order to test this prediction, we performed extensive numerical simulations in the particular case of the double-Morse potential [5]

$$V(q)=\left[\frac{\alpha-\cosh(bq)}{\alpha-1}\right]^2, \tag{14}$$

where the parameter $\alpha=\cosh(bq_0)$ determines the potential minima $q=\pm q_0$ ($q_1=-q_0$ and $q_2=q_0$). The explicit standing soliton solution is given by

$$\tanh\frac{bq_K}{2}=\pm\left(\frac{\alpha-1}{\alpha+1}\right)^{1/2}\tanh\frac{x}{d}, \tag{15}$$

with the soliton width

$$d=\frac{1}{b}\left(\frac{2(\alpha-1)}{\epsilon_0(\alpha+1)}\right)^{1/2}\gg 1. \tag{16}$$

The upper (lower) sign in Eq. (15) corresponds to the kink (antikink) solution. In the limiting case, when the parameter $b\to 0$, the double-well potential (14) becomes the well known ϕ^4 potential [2]: $V(q)=(1-q^2/q_0^2)^2$. The function $F(X)$ of Eq. (11) corresponding to the potential (14) is

$$F(X)=\frac{\sqrt{2\epsilon_0}(\alpha+1)}{\alpha-1+2\cosh^2(X/d)}. \tag{17}$$

The calculation of the rest soliton mass according to Eq. (10) yields

$$M_0=\frac{4}{b^2 d}\left(\frac{\alpha b q_0}{\sqrt{\alpha^2-1}}-1\right). \tag{18}$$

For the numerical solution of the Eqs. (2) we used the fourth-order Runge-Kutta method; for accuracy we monitored the total energy that was conserved to one part in 10^{-7}. The simulations have shown that for sufficiently small initial incoming velocities s_i's, smaller than a certain critical value s_{cr}, indeed, no *impurity modes* (see Sec. IV) are excited resulting in the predicted behavior, viz. $s_f=s_i$ [Fig. 1(a)]. Furthermore, random kink velocity fluctuations appear exactly as predicted by Eq. (13). As a result, the numerical simulations corroborate the picture furnished by Eq. (13) for kink propagation in a long mass-disordered medium in the velocity range $s_i<s_{cr}$.

The kink propagation picture in the fully disordered chain changes drastically for incoming kink velocities larger than the critical velocity s_{cr}. In this regime, the impurity modes are excited at the expense of the kink kinetic energy and, as a result, there is now a *reduction* in the exiting kink velocity s_f leading to the inequality $s_f<s_i$. This situation is illustrated in Fig. 1(b). To see if this picture appears also when *lighter impurities* are present in the disordered segment, we performed numerical simulations with impurity masses smaller than m_p, i.e., ''attractive impurities.'' We found that at large velocities kinks excite the impurities, loose energy, and depart with a smaller velocity. At small injection velocities, the exit kink velocity is again the same as the initial velocity; there is a similar yet *reversed* small velocity fluctuating pattern compared to that in Fig. 1(a), where the velocity fluctuations are now above the kink injection velocity. This is exactly the behavior predicted by Eq. (13). In order to treat the large velocity cases in the context of the collective coordinate formalism, we must introduce additional functions describing the amplitude of the impurity modes. The resulting dynamical system, even for the single impurity case, is quite complicated and will be studied in the Sec. IV.

We carried out numerical simulations for the calculation of the critical velocity s_{cr} and its dependence from the length of disordered segment. In Fig. 2(a) we show the results of a kink injected in a disordered chain consisting of 1000 units, by plotting the exiting kink velocity as a function of the incoming velocity. We observe equality at small velocities

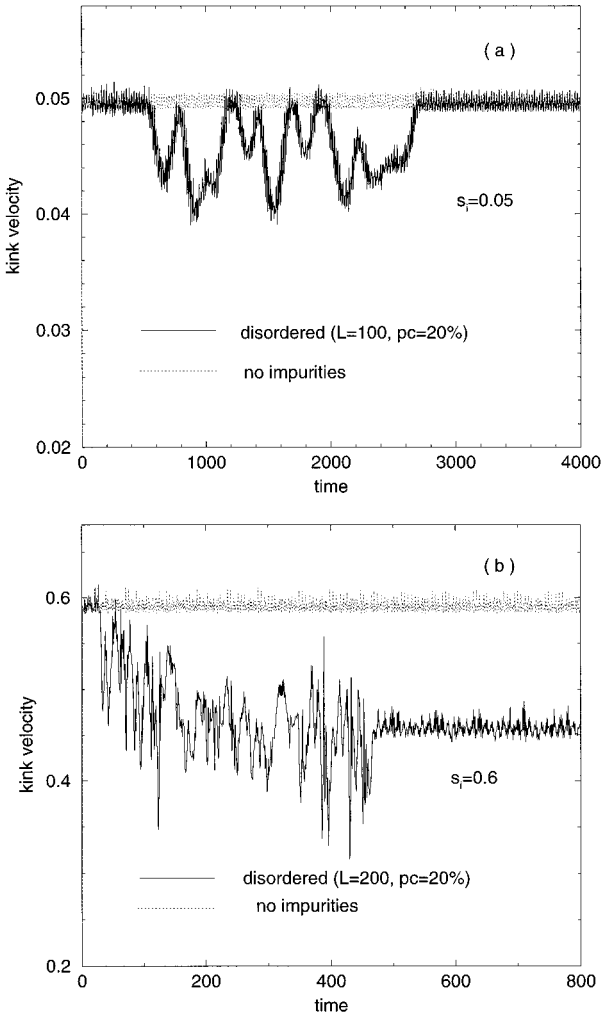

FIG. 1. Kink propagation in ordered and disordered media. For all the simulations we used for the on-site potential, that is given from Eqs. (1) and (14), values of the parameters $b=7$, $q_0=0.35$ and $\epsilon_0=0.005$. The sound velocity in the perfect chain is unity. (a) Kink propagation with small initial velocity $s_i=0.05$ for an ordered (dotted line) and a disordered (continuous line) HB chain consisting of 100 units with deuterium substitution pc equal to 20%. We observe here, as well as in simulations with much longer chains, that the kink exits with the same velocity even though its velocity has been fluctuating while in the disordered chain. (b) Similarly for large initial velocity $s_i=0.6$ and disordered segment of 200 unit cells. All quantities are dimensionless.

and departure from it after some critical value s_{cr}. In Fig. 2(b) we investigate the dependence of the critical velocity s_{cr}, operationally defined as the point of departure from the equality $s_i=s_f$ in Fig. 2(a), as a function of disordered length segment. We see that as the segment length increases, there is a clear saturation to a segment length independent value, approximately equal to $s_{cr}\approx 0.2$ (in units of sound velocity). As a result of our finding that for incoming kink velocities s_i's larger than some critical velocity s_{cr} kink energy losses commence, we expect that propagation in long disordered mesoscopic chains with many impurities will exhibit an effective maximal propagation velocity determined by s_{cr}. When a kink moves initially faster than this maximal veloc-

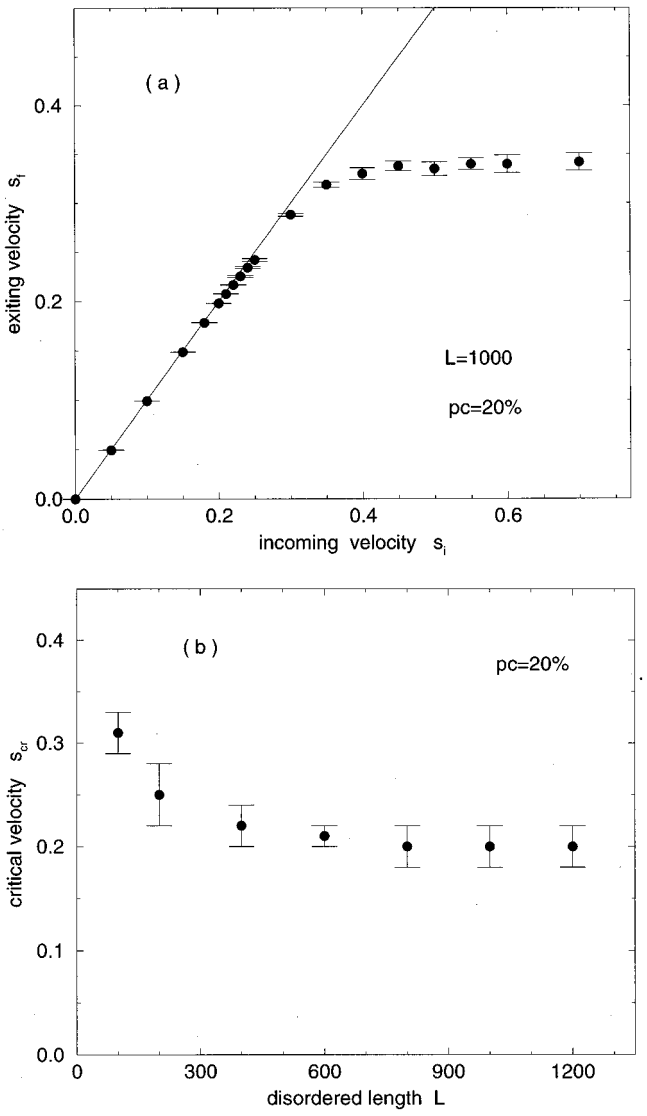

FIG. 2. (a) Exiting kink velocity as a function of incoming velocity for a disordered segment of 1000 units consisting of 20% mass impurity substitution. The error bars are error estimates taken from statistics with the chain configurations. We observe that the equality between incoming and exiting kink velocities starts departing at some critical velocity s_{cr}. (b) Critical velocity at which a measurable departure occurs from the equality $s_f = s_i$ as a function of disordered segment size. The deuterium content is at 20%.

ity, it excites impurity modes and by loosing energy, reduces its velocity until the maximal allowed velocity is reached; the latter is independent of the length of the disordered segment for very large lengths. In order to confirm this idea we performed additional numerical calculations for quite long disordered segments, shown in Fig. 3. Here, we injected a kink at a fixed initial velocity s_i much larger than s_{cr}, and register the exit velocity s_f for disordered segments of various lengths. We observe that the exit velocity drops very quickly as the segment size increases and subsequently approaches very slowly the asymptotic value $s_{cr} \approx 0.2$. We note also that Scr increases as the impurity concentration decreases.

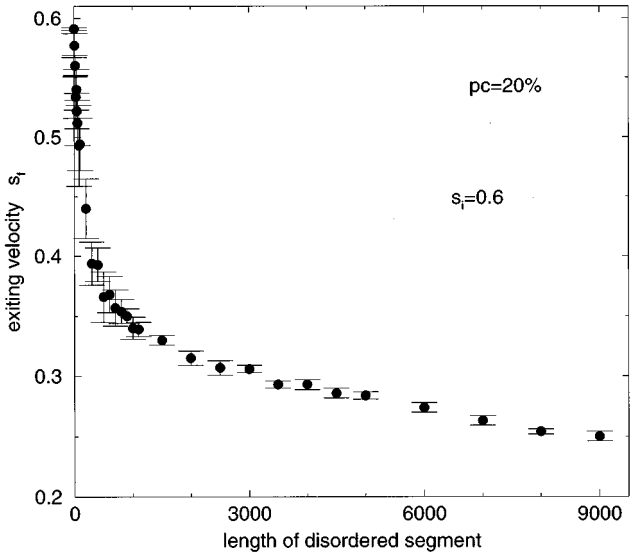

FIG. 3. Velocity of a kink exiting a disordered segment with 20% mass impurity substitution as a function of length size. The exiting velocity approaches slowly the limiting value $s_{cr} \approx 0.2$ at large disordered segment sizes. The initial velocity is 0.6. The error bars are error estimates taken from statistics with the chain configurations.

IV. SINGLE-IMPURITY MODE AND ITS INTERACTION WITH A KINK: COLLECTIVE COORDINATE APPROACH

When the density of deuterium atoms is low the average distance between adjacent impurities is larger than the soliton width. In this limit the scattering of a soliton by many impurities can approximately be treated independently, ignoring interference effects. Therefore, in order to understand the appearance of the soliton velocity threshold for values higher than that for which the soliton transparency through a mass-disordered segment is accompanied by energy losses, we consider an isolated impurity localized at a single site (e.g., at the site with $n=0$). We represent the relative mass variation along the chain as the sum

$$\mu_n = 1 + \eta \delta_{n,0}, \tag{19}$$

where η is the difference of the impurity mass and $\delta_{m,n}$ is the Kronecker symbol.

The impurity mode is the standing linear localized wave

$$q_n(\tau) = A_0 \exp(-|n|/\lambda)\cos(\Omega\tau) \tag{20}$$

with an arbitrary amplitude A_0. The two dimensionless quantities: correlation length λ and frequency Ω can be found explicitly [11] by substituting the ansatz (20) into the set of the linearized equations (2). Note that the similar procedure can be accomplished in the continuum limit [12–14]. The result is

$$\cosh\frac{1}{\lambda} = 1 + (\Omega_0^2 - \Omega^2)/2, \tag{21}$$

where $\Omega_0 = \sqrt{\epsilon_0 V''(\pm q_0)}$ is the dimensionless frequency of small-amplitude oscillations at each of the minima $q = \pm q_0$

and the impurity mode frequency Ω, depending on the impurity mass η, is given explicitly by (for $\eta>0$)

$$\Omega^2=\frac{\Omega_0^2+2-\sqrt{(\Omega_0^2+4)\Omega_0^2\eta^2+4}}{1-\eta^2}. \tag{22}$$

When $\eta\to 0$ (the ''amplitude'' impurity vanishes), then $\Omega\to\Omega_0$ and $\lambda\to\infty$, i.e., the impurity mode is delocalized.

We can study the interaction of a moving kink (or antikink) with the impurity mode in the continuum limit ($n=x$) by using the collective coordinate approach. According to Eq. (20), we assume a general solution to be in the form of the linear superposition

$$q(x,\tau)=q_K(x-X(\tau))\pm A(\tau)\exp(-|x|/\lambda) \tag{23}$$

where the upper (lower) sign coincides with that of the kink (antikink) solution given implicitly by Eqs. (5) and (6) [see, also, Eq. (15)]. The function $A=A(\tau)$ describes the small-amplitude background for the kink (antikink). Note that in the case of absence of the interaction with the kink, we have $A(\tau)=A_0\cos(\Omega\tau)$ [see Eq. (20)]. Both the variables $X(\tau)$ and $A(\tau)$ are to be determined whereas the parameter λ is defined according to Eqs. (21) and (22).

After a series of calculations presented in the Appendix we arrive at the equations of motion for both the generalized coordinates $X(\tau)$ and $A(\tau)$

$$\begin{aligned}&[M_0+\eta F^2(X)]\ddot{X}-\eta F^3(X)G(X)\dot{X}^2-[I(X)+\eta F(X)]\ddot{A}\\&\quad+J'(X)A^2/2=0,\\&(\lambda+\eta)(\ddot{A}+\Omega^2A)-[I(X)+\eta F(X)]\ddot{X}\\&\quad-[I'(X)-\eta F^2(X)G(X)]\dot{X}^2+J(X)A=0,\end{aligned} \tag{24}$$

where the function G is defined by $G(x)=-F'(x)/F^2(x)$ while the functions I and J and the derivatives I' and J' are given in the Appendix.

The set of Eqs. (24) describes the interaction of the effective particle, the position of which is given by the coordinate $X(\tau)$, with the oscillator $A(\tau)$ situated at the origin $x=0$. This interaction is completely determined by the shape of the potential function $F(X)$, i.e., by the profile of the soliton solution $q_K'(x)$ [see Eq. (11)]. The other function $G(x)$ and the convolutions $I(X)$ and $J(X)$ are given in terms of the potential $F(x)$. In the limiting case $\eta\to 0$ ($\Omega\to\Omega_0$ and $\lambda\to\infty$), when $I(X)\to I_0=$ const and $J(X)\to J_0=$ const, the equations of motion (24) are reduced to

$$M_0\ddot{X}-I_0\ddot{A}=0,\quad \ddot{A}+\Omega_0^2A=0. \tag{25}$$

These equations describe the interaction of the soliton with the infinitely extended harmonic wave of the frequency Ω_0. Their integration yields the soliton motion consisting of two parts: uniform (depending on the initial conditions) and oscillating (with the frequency Ω_0).

The results of integration of the effective equations (24) in the framework of the collective coordinate approximation (CCA) and their comparison with those of the direct simulations of the basic equations of motion (2) with one deuterium impurity, are presented in Figs. 4 and 5. It follows from these figures that the results of the CCA are in good correspondence with the direct simulation results. Thus, both pictures (direct and collective coordinate) illustrate that no impurity modes are excited and, as a result, $s_f=s_i$ if initial velocities are sufficiently small. It was fascinating to observe that during the kink passage in the vicinity of the impurity, the oscillator coordinate (the displacement of the deuterium from its equilibrium position) $A(\tau)$ displaces forward and backwards accomplishing in time approximately just one oscillation period, as shown in Fig. 5. The amplitude of this one-period oscillation increases with the growth of initial velocity. For higher incoming velocities nonvanishing (residual) impurity oscillations appear. The amplitude of these oscillations is much smaller than the displacement pulse (one-period oscillation) appearing and existing during the kink-impurity interaction. As the initial velocity s_i increases the amplitude of the residual oscillations becomes larger. After the kink-impurity interaction terminates, the oscillation amplitude is stabilized to some constant value. In other words, above the critical velocity, there is some energy loss of the incoming soliton resulting in decreasing its velocity. Therefore, the residual oscillations can be referred to as the impurity mode. Since these results, at least at the qualitative level, coincide with those of the direct simulations of Eqs. (2), one can conclude that the collective coordinate approximation adequately describes the scattering picture of a soliton by a mass impurity.

In Fig. 6 we plot the energy of the impurity mode, a long time after the passage of the kink from the impurity site, as a function of the initial kink velocity. For the case of the direct simulation of the equations of motion (2) we calculate the impurity mode energy using Hamiltonian (1), where the sum extends to a segment of 2λ sites to the left to 2λ sites to the right of the impurity site [see Fig. 6(a)]. For the case of CCA we plot the energy of oscillator given by the expression $(\lambda+\eta)(\dot{A}^2+\Omega^2A^2)/2$ [see Fig. 6(b)]. These figures demonstrate a behavior similar of that depicted in Fig. 2(a), i.e., for small initial kink velocities we have $s_f=s_i$ and for larger ones we have $s_f<s_i$. However, in the CCA scheme [Fig. 6(b)] we see that some form of ''modulation'' takes place; there are two abrupt drops beginning at $s_i\simeq 0.4$ and $s_i\simeq 0.6$, that are not expected and, more importantly, not confirmed by the direct simulation picture given in Fig. 6(a). This discrepancy can be explained by the fact that we have adopted the particle-oscillator approximation, assuming Eqs. (7) valid only for sufficiently small velocities. The resulting particle-oscillator system described by the equations of motion (24) appears to be a crude approximation to the many-oscillator system governed by Eqs. (2). A simplified system of equations, such as Eqs. (24), with only *two degrees of freedom*, has some nonlinear resonance properties which are exhibited by the modulated behavior. In order to improve this approximation the collective coordinate scheme applied in this paper would have to be developed in a more precise way by taking into account the relativistic behavior, and instead of Eqs. (7) taking exact derivatives of $q=q_K(\xi)$, viz. $q_\tau=-\gamma\dot{X}(1-\gamma\ddot{X}\xi)q_K'(\xi)$, $q_x=\gamma q_K'(\xi)$ where $\xi\equiv\gamma(x-X)$ and $\gamma=(1-\dot{X}^2)^{-1/2}$. However, the resulting effective equations of motion become very complicated and their analysis is much more difficult.

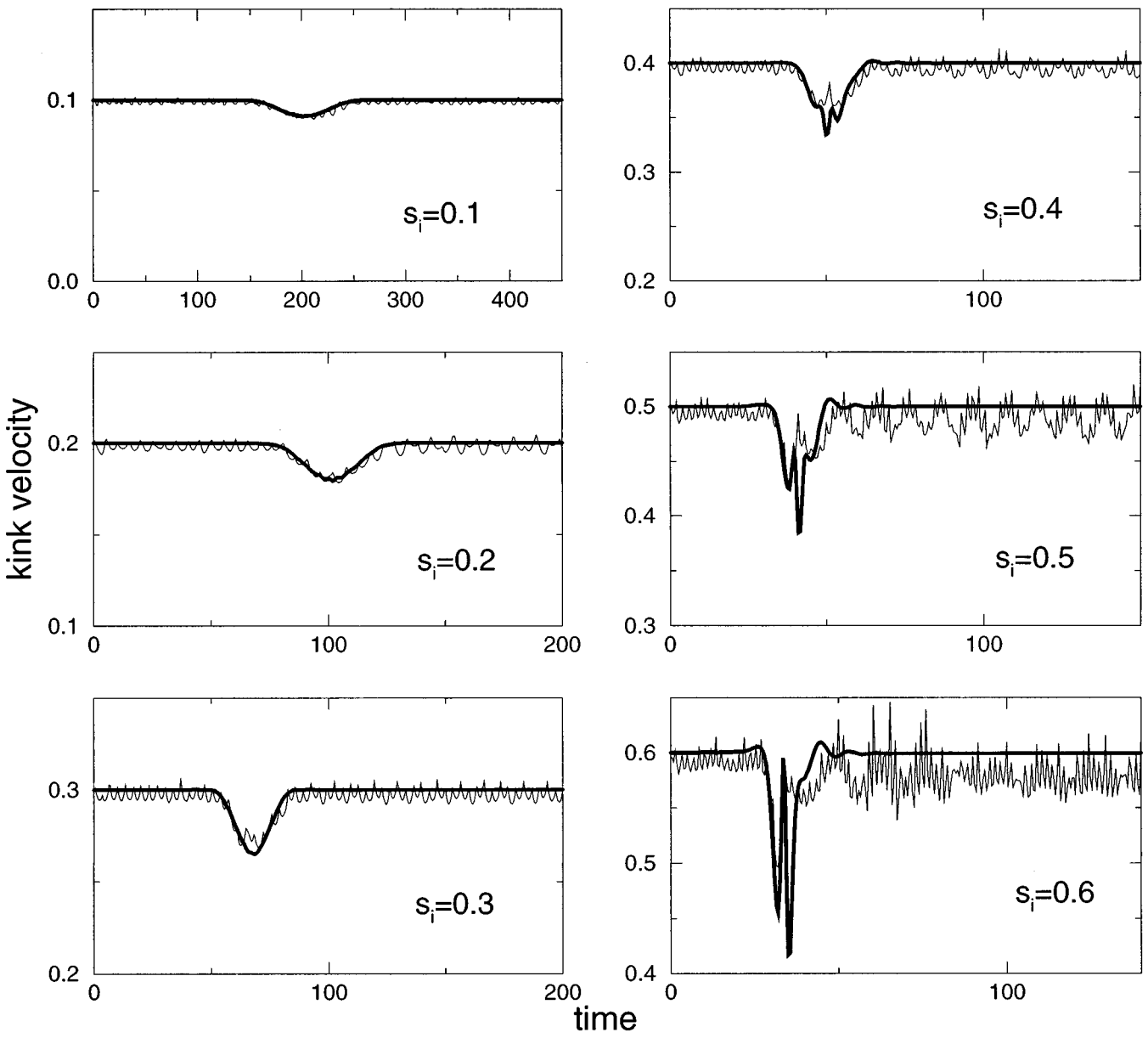

FIG. 4. Propagating kink velocity (ordinate) as a function of time (abscissa) for kinks with different initial velocities s_i. When the kink interacts with a deuterium impurity its velocity drops. The thick lines show the results of the collective coordinate approximation while thin lines show the direct simulations of the equations of motion (2).

V. SUMMARY

We have examined the propagation of proton solitons (kinks and antikinks) in isotopically random chains and found that, contrary to intuition, impurity modes are not excited for low (compared to s_{cr}) incoming velocity of the soliton (at least such an excitation was not detected within the accuracy of our numerical simulation). In contrast, at relatively high velocities the soliton loses part of its energy and slows down. Since in the absence of mass variation the soliton propagates perfectly at these velocities, we conclude that its loss of energy is directly attributed to the excitation of the impurity modes in a mass-disordered segment of the chain. Since the same exit velocity reduction is not observed at low velocities, it is evident that the impurity modes are not excited then. These effects of the *absence of excitation of the impurity modes* at small velocities and their appearance at a certain critical incoming velocity are clearly depicted in Fig. 2(a) where we plot the kink velocity after exiting the disordered segment as a function of the incoming velocity in the 1000 site long disordered segment. This also appears in the scattering of a kink by a single impurity, where the impurity mode is not excited for sufficiently small initial kink velocities. The existence of an upper critical propagation soliton velocity s_{cr} in the mass-disordered medium that is lower than the speed of sound in the perfect lattice signifies that the effective proton motion is much slower when deuterium impurities are present in an HB chain. This phenomenon of the effective renormalization of the maximal propagation kink velocity in the presence of disorder could be used experimentally for the assessment of the nonlinear aspects of the proton dynamics.

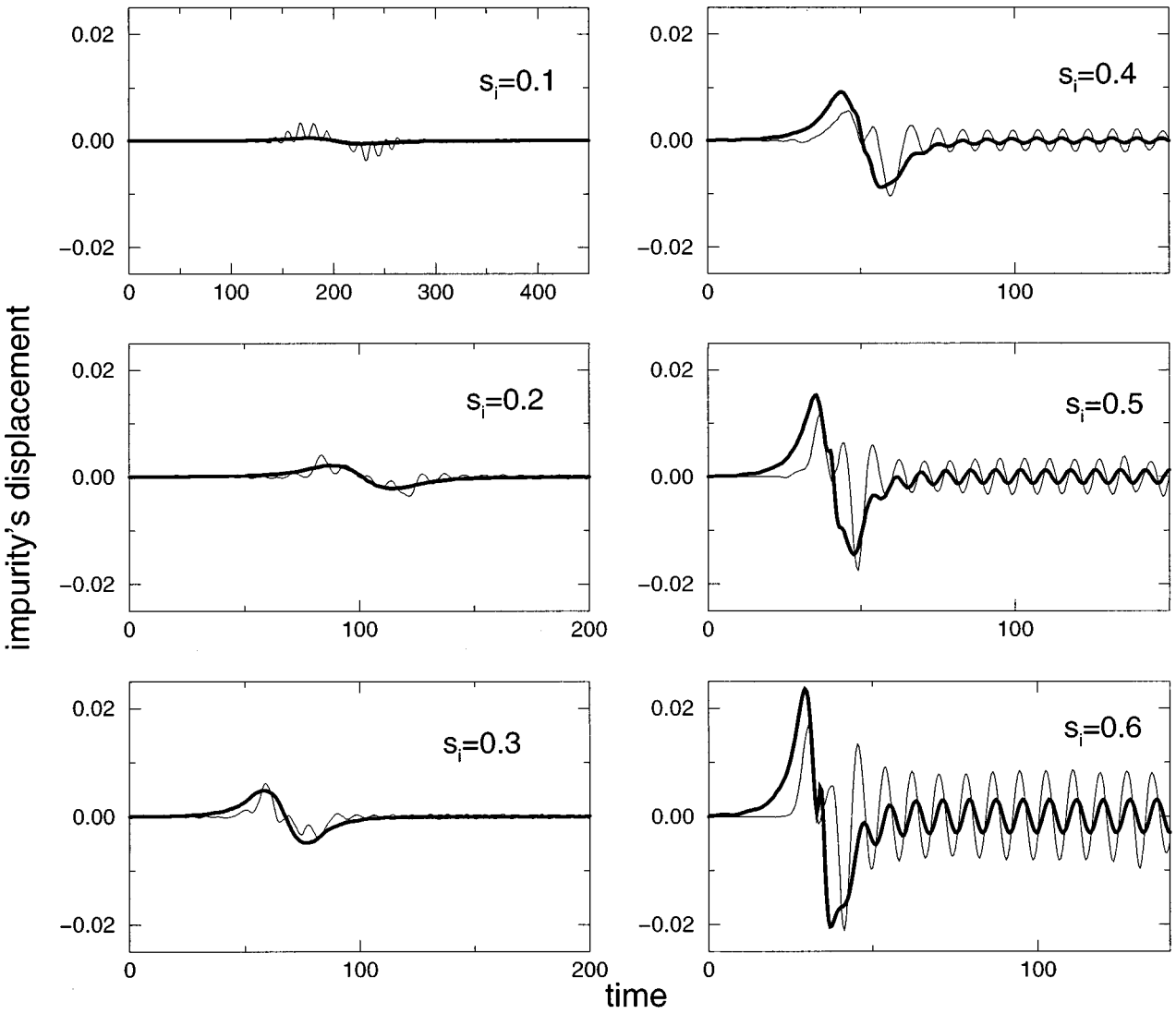

FIG. 5. Deuterium impurity displacement from the minimum of the on-site potential as a function of time, for different initial kink velocities s_i. The deviation from the zero value is a result of the passage of the kink through the impurity. The thick lines show the results of the collective coordinate approximation while the thin lines show the direct simulations of the equations of motion (2).

ACKNOWLEDGMENTS

Stimulating and useful discussions with Professor G. Careri on experimental aspects of HB systems are gratefully acknowledged. We thank M. Xilouris, S. Komineas, and N. Lathiotakis for computational assistance. The work was supported from INTAS Grant No. 94-3754, HCM Grant No. ERB-CHRX-CT93-0331 of the European Community and ΠΕΝΕΔ Grant No. 95 EΔ 115 of the General Secretariat for Research and Technology of Greece.

APPENDIX

Upon substitution of the ansatz (23) as well as the continuum form of Eq. (19), viz. $\mu(x)=1+\eta\delta(x)$, where $\delta(x)$ is the Dirac δ function, into the Lagrangian (3) and using Eqs. (7), (9)–(11), and $F(-x)=F(x)$, in the nonrelativistic limit we find the effective Lagrangian (up to a constant)

$$\mathcal{L}(X,\dot{X};A,\dot{A}) \simeq \tfrac{1}{2}(M_0+\eta F^2)\dot{X}^2-(I+\eta F)\dot{X}\dot{A} + \tfrac{1}{2}(\lambda+\eta)(\dot{A}^2-\Omega^2A^2)-\tfrac{1}{2}JA^2, \quad \text{(A1)}$$

where

$$I(X)=\int F(x-X)\exp(-|x|/\lambda)dx, \quad \text{(A2)}$$

$$J(X)=\int \{\epsilon_0 V''[q_K(x-X)]-\Omega_0^2\}\exp(-2|x|/\lambda)dx. \quad \text{(A3)}$$

In the calculations of the Lagrangian (A1), we have expanded the function $V(q)$ in the vicinity of the soliton solution $q_K(x-X)$ up to the second order and then we used the relation $(\lambda+\eta)\Omega^2=\lambda^{-1}+\lambda\Omega_0^2$ which follows from Eqs.

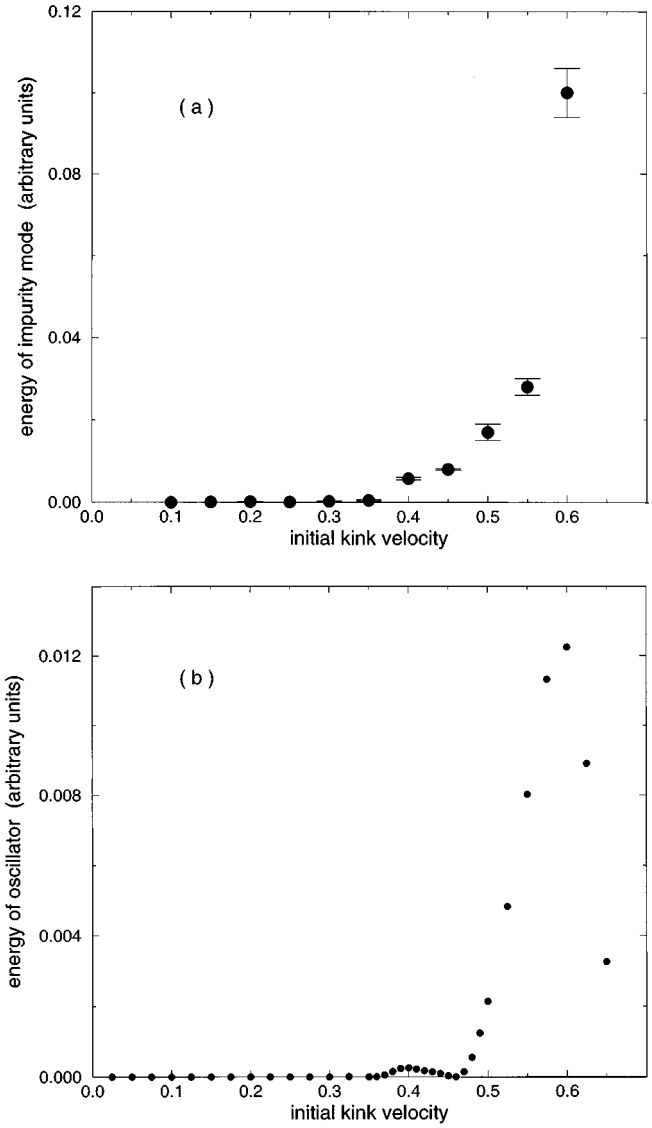

FIG. 6. Energy of the impurity mode long time after the passage of the kink from the impurity site as a function of the initial kink velocity. In (a) we present results from the direct simulation of the equations of motion (2) and in (b) results in the framework of the collective coordinate approximation.

(21) and (22). In the limit $A(\tau)\rightarrow 0$ the effective Lagrangian (A1) is reduced to the form (8), so that Eq. (13) can be rewritten as

$$\dot{X}=\frac{s_i}{\pm\sqrt{1+(\eta/M_0)F^2(X)}} \tag{A4}$$

if we substitute there $\delta\mu(x)=\eta\delta(x)$. We have inserted the sign ''$\pm$'' in Eq. (A4) because when the mass impurity η is very large (compared to deuterium) and the initial kink velocity larger than a threshold value, the kink reflection takes place [23].

From the Lagrangian (A1) result the equations of motion (24) for the generalized coordinates $X(\tau)$ and $A(\tau)$, that describe the system in the framework of the collective coordinate approximation. Using the expression $G(x)=-F'(x)/F^2(x)$ we have

$$I'(X)=\int F^2(x-X)G(x-X)\exp(-|x|/\lambda)dx, \tag{A5}$$

$$J(X)=\int\{F(x-X)[2F(x-X)G^2(x-X)-G'(x-X)]-\Omega_0^2\}\exp(-2|x|/\lambda)dx, \tag{A6}$$

$$J'(X)=\int F(x-X)[4F^2(x-X)G^3(x-X)-5F(x-X)\times G(x-X)G'(x-X)+G''(x-X)]\times\exp(-2|x|/\lambda)dx. \tag{A7}$$

The system of coupled equations (24) can be transformed in a form convenient for numerical integration and solve them using the boundary conditions $X(-\infty)=-\infty$, $\dot{X}(-\infty)=s_i$, $A(-\infty)=0$, $\dot{A}(-\infty)=0$. We choose the potential of Eq. (14) for our numerical simulations; as a result the function $F(X)$ is given by Eq. (17), while the $G(X)$ is

$$G(X)=\frac{b}{\sqrt{\alpha^2-1}}\sinh(2X/d). \tag{A8}$$

The calculation of the frequency of small-amplitude oscillations yields $\Omega_0=\sqrt{\epsilon_0 V''(\pm q_0)}=2/d$. For the numerical solution of the Eqs. (24), besides Eqs. (16), (17), (18), (A2) and (A5), we used the following specific form for the expressions (A6) and (A7), viz:

$$J(X)=-\frac{b^2}{\alpha+1}\int F^2(x-X)\left(\frac{6\alpha}{\alpha-1}\cosh^2\frac{x-X}{d}+\alpha-2\right)\times\exp\left(-\frac{2|x|}{\lambda}\right)dx,$$

$$J'(X)=-\frac{b^2}{\alpha+1}\int F^3(x-X)G(x-X)\times\left(\frac{6\alpha}{\alpha-1}\cosh^2\frac{x-X}{d}-\alpha-4\right)\exp\left(-\frac{2|x|}{\lambda}\right)dx. \tag{A9}$$

[1] J. F. Nagle, M. Mille, and H. J. Morowitz, J. Chem. Phys. **72**, 3959 (1980).
[2] S. Aubry, J. Chem. Phys. **62**, 3217 (1975); J. A. Krumhansl and J. R. Schrieffer, Phys. Rev. B **11**, 3535 (1975).
[3] J. F. Currie, S. E. Trullinger, A. R. Bishop, and J. A. Krumhansl, Phys. Rev. B **15**, 5567 (1977).
[4] A. R. Bishop, J. A. Krumhansl, and S. E. Trullinger, Physica D **1**, 1 (1980).
[5] See, e.g., A. V. Zolotaryuk, St. Pnevmatikos, and A. V. Savin, Physica D **51**, 407 (1991); X. Duan and S. Scheiner, J. Mol. Struct. **270**, 173 (1992).
[6] St. Pnevmatikos, Phys. Rev. Lett. **60**, 1534 (1988).

[7] G. P. Tsironis and St. Pnevmatikos, Phys. Rev. B **39**, 7161 (1989).
[8] A. V. Zolotaryuk and St. Pnevmatikos, Phys. Lett. A **143**, 233 (1990).
[9] St. Pnevmatikos, G. P. Tsironis, and A. V. Zolotaryuk, J. Mol. Liq. **41**, 85 (1989).
[10] Q. Li, St. Pnevmatikos, E. N. Economou, and C. M. Soukoulis, Phys. Rev. B **37**, 3534 (1988).
[11] T. Fraggis, St. Pnevmatikos, and E. N. Economou, Phys. Lett. A **142**, 361 (1989).
[12] Yu. S. Kivshar, Phys. Rev. A **43**, 3117 (1991).
[13] O. M. Braun and Yu. S. Kivshar, Phys. Rev. B **43**, 1060 (1991).
[14] Z. Fei, Yu. S. Kivshar, and L. Vázquez, Phys. Rev. A **45**, 6019 (1992).
[15] M. Imada, J. Phys. Soc. Jpn. **52**, 179 (1983).
[16] Q. Li, C. M. Soukoulis, St. Pnevmatikos, and E. N. Economou, Phys. Rev. B **38**, 11 888 (1988).
[17] Yu. S. Kivshar, S. A. Gredeskul, A. Sánchez, and L. Vázquez, Phys. Rev. Lett. **64**, 1693 (1990).
[18] S. Takeno and S. Homma, J. Phys. Soc. Jpn. **60**, 731 (1991).
[19] S. A. Gredeskul and Yu. S. Kivshar, Phys. Rep. **216**, 1 (1992).
[20] V. V. Konotop, Phys. Rev. E **50**, 2600 (1994).
[21] G. Careri, F. Bruni, and G. Consolini, in *Nonlinear Quasiparticles in Biology*, edited by M. Peyrard (Springer, Paris, 1995).
[22] D. W. McLaughlin and A. C. Scott, Phys. Rev. B **18**, 1652 (1978).
[23] Similar results regarding the reflection were obtained in Ref. [14] for the case of a sine-Gordon kink impinging on a single repulsive mass impurity.